

Phase Equilibria of Semiclathrate Hydrates of CO₂, N₂, CH₄, or H₂ + Tetra-*n*-butylammonium Bromide Aqueous Solution

Amir H. Mohammadi,^{*,†,‡} Ali Eslamimanesh,[†] Veronica Blandria,[†] and Dominique Richon[†]

[†]MINES ParisTech, CEP/TEP - Centre Énergétique et Procédés, 35 Rue Saint Honoré, 77305 Fontainebleau, France

[‡]Thermodynamics Research Unit, School of Chemical Engineering, University of KwaZulu-Natal, Howard College Campus, King George V Avenue, Durban 4041, South Africa

ABSTRACT: Semiclathrate hydrate dissociation conditions measured for the systems including CO₂, N₂, CH₄, or H₂ + tetra-*n*-butylammonium bromide (TBAB) aqueous solution with a wide range of concentrations (0.050, 0.100, 0.150, 0.153, 0.167, 0.250, 0.350, and 0.500 mass fraction) are reported. These data were measured in a (277.7 to 294.7) K temperature range and pressures up to 15.49 MPa pursuing an isochoric pressure search method. Some comparisons are made between our data and the experimental phase equilibrium data reported in open literature. The comparisons show that some literature data seem to be not reliable.

1. INTRODUCTION

Fossil fuels, for example, coal, oil, and natural gas are increasingly consumed by population growth and energy demands.^{1–5} Several comprehensive studies demonstrate that too much carbon dioxide, carbon monoxide, hydrogen sulfide, and methane (called “greenhouse gases”) are emitted every year to the atmosphere.^{1–5} Some of the major concerns of excess concentration of these gases in the Earth's atmosphere are the global climate change and interference in ocean biochemistry, which contribute to consequent inevitable unpleasant universal effects including a rise in sea levels, increase of probability of skin cancer, global warming, and harmful effects on living organisms such as the ones associated with the human beings.^{1–6}

In general, CO₂ emissions to the atmosphere can be decreased through energy intensity reduction, carbon intensity reduction, and the CO₂ capture and sequestration (CCS).⁷ The CCS has become an important area of research to mitigate CO₂ worldwide emissions because around 64% of the greenhouse gas effects are related to carbon dioxide emissions.^{1–9} Since CO₂ separation is the most expensive step of the CCS^{7–15} process, the challenge is to innovate energy-efficient and environmentally friendly technologies to capture the CO₂ produced in large scale power-plants, where flue gas typically contains mostly N₂ and CO₂.^{1–16} However, halting the increase in CO₂ emissions by transitioning to nonfossil energy use is not compatible with energy demand, which certainly tends to increase rather than decrease in the coming years, especially in developing countries.⁶ Therefore, searches must be done for alternative techniques for this purpose.

On the other hand, N₂ is known as one of the major components of flue gas emitted from powerplants including electric power, fertilizer, and cement plants, and so on.^{8,16,17} Furthermore, N₂ forms a main portion of the atmosphere. Therefore, considerable industrial data (including phase equilibrium data) are required for investigating the behavior of this component not only in its corresponding separation process but also during CO₂ capture techniques.

Methane is also a greenhouse gas with a greenhouse effect of 21 times stronger than that of CO₂, and it contributes to 18 % of

the global greenhouse effect.^{17–20} It remains in the atmosphere for approximately (9 to 15) years. This component constitutes a main part of natural gas streams, natural gas reserves in the form of hydrates in the earth. It is emitted also from agricultural activities, coal mining, stationary and mobile combustion, wastewater treatment, and in the form of cold bed methane (CBM) discharging from coal seams.^{17–23} The historical record, based on an analysis of air bubbles trapped in ice sheets, indicates that methane is more abundant in the Earth's atmosphere now than at any time during the past 400 000 years.²⁴ Over the last two centuries, methane concentrations in the atmosphere have more than doubled.²⁴ Regarding these facts, the separation of methane from industrial gas flows (or simultaneously with CO₂ capture process) has been of significant attention in the past decade. For instance, particular amounts of CO₂ should be removed from natural gas streams, in which the main component is methane, to elevate the quality of the gas and reach the desired residual values, such as preventing corrosion in the pipelines and processes facilities and also enhancing the heat value of the gas streams.

Moreover, hydrogen, as a clean and novel energy resource, has generated numerous discussions recently. The separation, storage, and transportation of this component are among new industrial technologies.^{10,17}

One promising approach, in comparison with the cryogenic distillation, membrane purification, and absorption with liquids, to separate carbon dioxide (and consequently other components) from combustion flue gas streams is through a gas hydrate crystallization technique.^{1,8–18,25} Gas hydrates, or clathrate hydrates, are a group of nonstoichiometric, ice-like crystalline compounds formed through a combination of water and suitably sized “guest” molecule(s), so-called “hydrate former(s)”, under low temperatures and elevated pressures.^{25,26} In the clathrate hydrate lattice, water molecules form hydrogen-bonded cage-like structures, encapsulating the guest molecules or hydrate former(s),

Received: May 26, 2011

Accepted: July 13, 2011

Published: August 26, 2011

Table 1. Experimental Data Available in Open Literature for Semiclathrate Hydrates of the Carbon Dioxide + TBAB Aqueous Solution System

authors	w_{TBAB}^a	T^b		N^d
		K	MPa	
Duc et al. ¹⁴	0.05, 0.10, 0.4, 0.65	(279.3 to 290.9)	(0.273 to 3.320)	8
Arjmandi et al. ⁴⁷	0.10, 0.427	(285.6 to 291.2)	(1.250 to 4.090)	7
Oyama et al. ⁴⁸	0.01, 0.02, 0.03, 0.045, 0.10	(276.7 to 289.55)	(0.560 to 4.530)	44
Lin et al. ⁴⁹	0.901, 0.702, 0.443	(279.4 to 288.1)	(0.344 to 2.274)	24
Deschamps and Dalmazzone ³⁸	0.40	(286.5 to 288.6)	(0.830 to 2.250)	4
Li et al. ⁵⁰	0.05, 0.10	(280.2 to 288.8)	(0.400 to 3.210)	11

^a Concentration (mass fraction). ^b Temperature. ^c Pressure. ^d Number of data points.

Table 2. Experimental Data Available in Open Literature for Semiclathrate Hydrates of the Nitrogen + TBAB Aqueous Solution System

authors	w_{TBAB}^a	T^b		N^d
		K	MPa	
Arjmandi et al. ⁴⁷	0.10	(285.15 to 292.95)	(4.688 to 33.503)	7
Duc et al. ¹⁴	0.05, 0.10	(279.3 to 284)	(2.900 to 10.850)	3
Deschamps and Dalmazzone ³⁸	0.40	(284.8 to 291.6)	(0.000 to 205)	6
Lee et al. ¹⁶	0.50, 0.20, 0.4, 0.60	(281.3 to 289.4)	(4.040 to 9.490)	19

^a Concentration (mass fraction). ^b Temperature. ^c Pressure. ^d Number of data points.

Table 3. Experimental Data Available in Open Literature for Semiclathrate Hydrates of the Methane + TBAB Aqueous Solution System

authors	w_{TBAB}^a	T^b		N^d
		K	MPa	
Li et al. ⁵⁰	0.05, 0.099, 0.197, 0.385	(281.15 to 295.15)	(0.460 to 10.640)	40
Arjmandi et al. ⁴⁷	0.05, 0.10, 0.2, 0.30	(287.15 to 298.15)	(1.421 to 41.369)	24
Oyama et al. ⁴⁸	0.10	(282.15 to 287.95)	(0.510 to 3.650)	7
Mohammadi and Richon ⁵¹	0.05	(283.6 to 290.1)	(1.310 to 11.080)	10
Sun and Sun ⁵²	0.05, 0.1, 0.2, 0.2818, 0.45	(281.75 to 292.35)	(0.508 to 7.042)	40

^a Concentration (mass fraction). ^b Temperature. ^c Pressure. ^d Number of data points.

which generally consist of low molecular diameter gases and organic compounds.^{25,26} The common gas hydrate crystalline structures are structure I (sI), structure II (sII), and structure H (sH), where each structure is composed of a certain number of cavities formed by water molecules.^{25,26} A concise review of gas hydrates is given elsewhere.²⁵

On the basis of the difference in chemical affinity between CO₂ and other gases (N₂, CH₄, and H₂) in the hydrate structure, when hydrate crystals are formed from a binary mixture of the aforementioned gases, the hydrate phase is enriched in CO₂ while the concentration of other gases is increased in the gas phase at equilibrium.⁹ The hydrate phase is then dissociated by depressurization or heating; consequently, CO₂ can be recovered as a separated gas.^{1,8–18,25}

For instance, applying gas hydrate formation processes, a double-effect process can be designed to replace the current pressure swing adsorption (PSA) method to capture CO₂ and H₂ separation simultaneously from the generated gas stream after steam reforming operation.^{10,17} Extremely high pressures [(100 to 360) MPa]^{10,17,27} are needed to stabilize the sII H₂

clathrate hydrate; however, CO₂ is enclathrated in hydrate cages at moderate pressure conditions.^{10,17,27} The difference between hydrate formation pressures of these two substances determines the potential of application of gas hydrate technology for the mentioned process.^{10,17,27}

Furthermore, gas hydrate promoters have been generally considered as additives to the hydrate crystallization processes to greatly reduce the required hydrate formation pressure and increase the formation rate or temperature along with modification of the selectivity of hydrate cages for absorption of various gas molecules in the water cages. The nowadays gas hydrate formation promoters can be categorized into two distinct groups: (1) chemical additives that have no effect on the structures of the water cages, for example, tetrahydrofuran (THF), anionic or nonionic surfactants, cyclopentane, acetone, and others;^{17,28–34} and (2) ones which change the structures of the ordinary water cages in the traditional clathrates structures such as tetra-*n*-butylammonium salts and [(*n*-C₄H₉)₄NBH₄].^{17,35–40} THF, from the first group, and TBAB (tetra-*n*-butylammonium bromide), from the second one, are the most famous thermodynamic

Table 4. Experimental Data Available in Open Literature for Semiclathrate Hydrates of the Hydrogen + TBAB Aqueous Solution System

author(s)	w_{TBAB}^a	T^b		N^d
		K	MPa	
Hashimoto et al. ⁵³	0.401	(285.4 to 287.3)	(0.130 to 13.60)	13
Arjmandi et al. ⁴⁷	0.10, 0.43	(280.15 to 288.00)	(3.600 to 23.070)	9
Oyama et al. ⁴⁸	0.15, 0.25	(282.95 to 284.57)	(0.630 to 5.840)	10
Hashimoto et al. ⁵⁴	0.975, 0.2674, 0.5783	(279.43 to 287.16)	(0.490 to 14.7)	28
Hashimoto et al. ⁵⁵	0.2674, 0.4074	(286.45 to 297.85)	(19.50 to 185)	12
Chapoy et al. ⁵⁶	0.37	(285.95 to 287.15)	(3.640 to 16.31)	4

^a Concentration (mass fraction). ^b Temperature. ^c Pressure. ^d Number of data points.

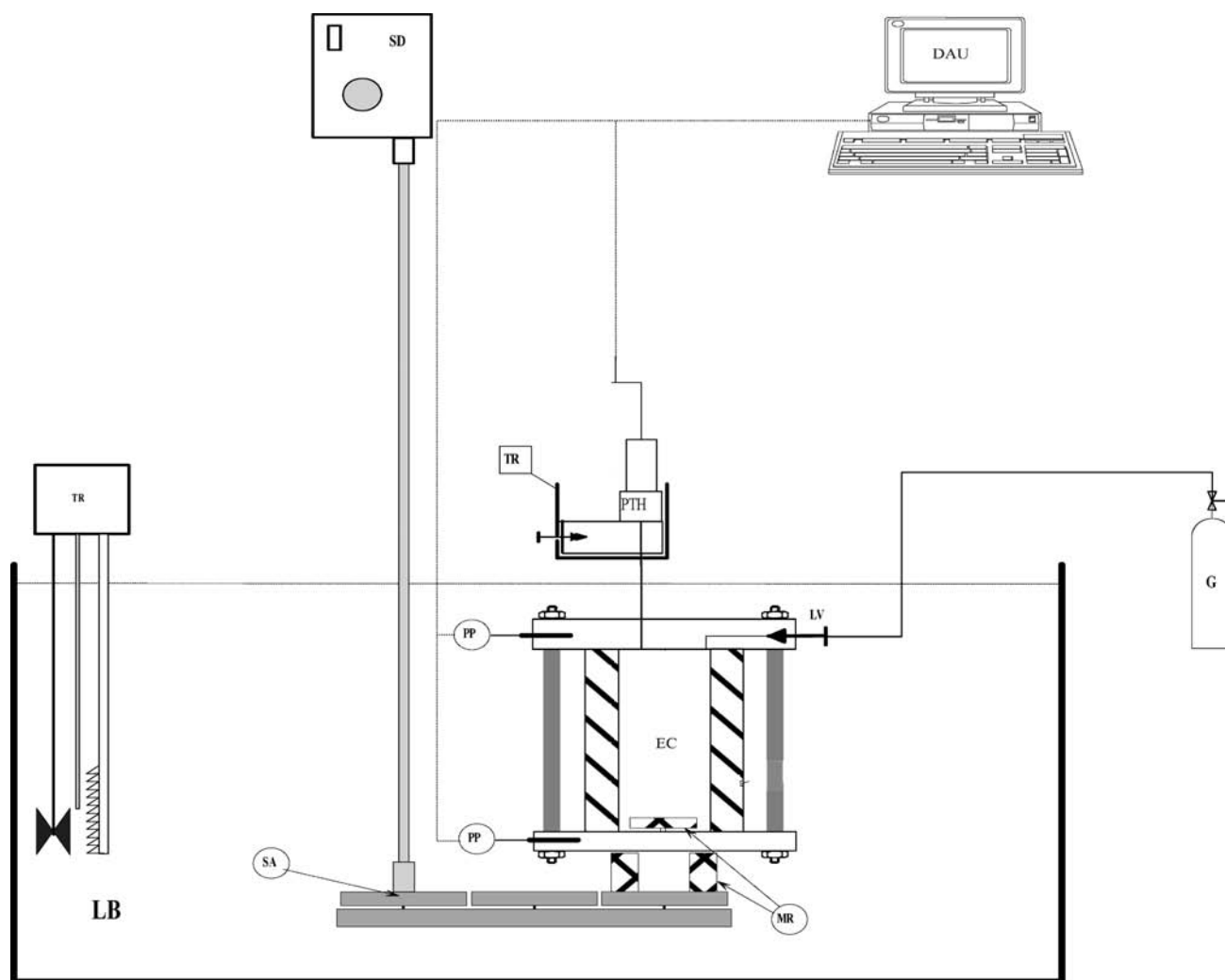


Figure 1. Schematic diagram of the experimental apparatus 1. DAU, data acquisition unit; EC, equilibrium cell; G, gas cylinder; LB, liquid bath; LV, loading valve; MR, magnetic rod; PP, platinum probe (temperature sensor); PTH, pressure transducer; SA, stirring assembly; SD, stirring device with variable speed motor; TR, temperature controller.

promoters that have been well-investigated in recent years. As a matter of fact, the second groups of promoters, mainly consisting of environmental friendly tetra-*n*-butylammonium salts, form semiclathrate hydrates, in which a part of the cage structure is broken to encage the large tetra-*n*-butylammonium molecule. This characteristic of the semiclathrate hydrates leads them to have more gas storage capacity than the promoters such as

THF. Although the promoters like THF can significantly decrease the hydrate formation pressure, they are unfortunately volatile. This fact results in greater losses during the corresponding storage, separation, and transportation processes than promoters forming semiclathrate hydrates.

Tables 1 to 4 show the reported phase equilibrium data so far for semiclathrate hydrates in the systems including CO₂, N₂, CH₄, and

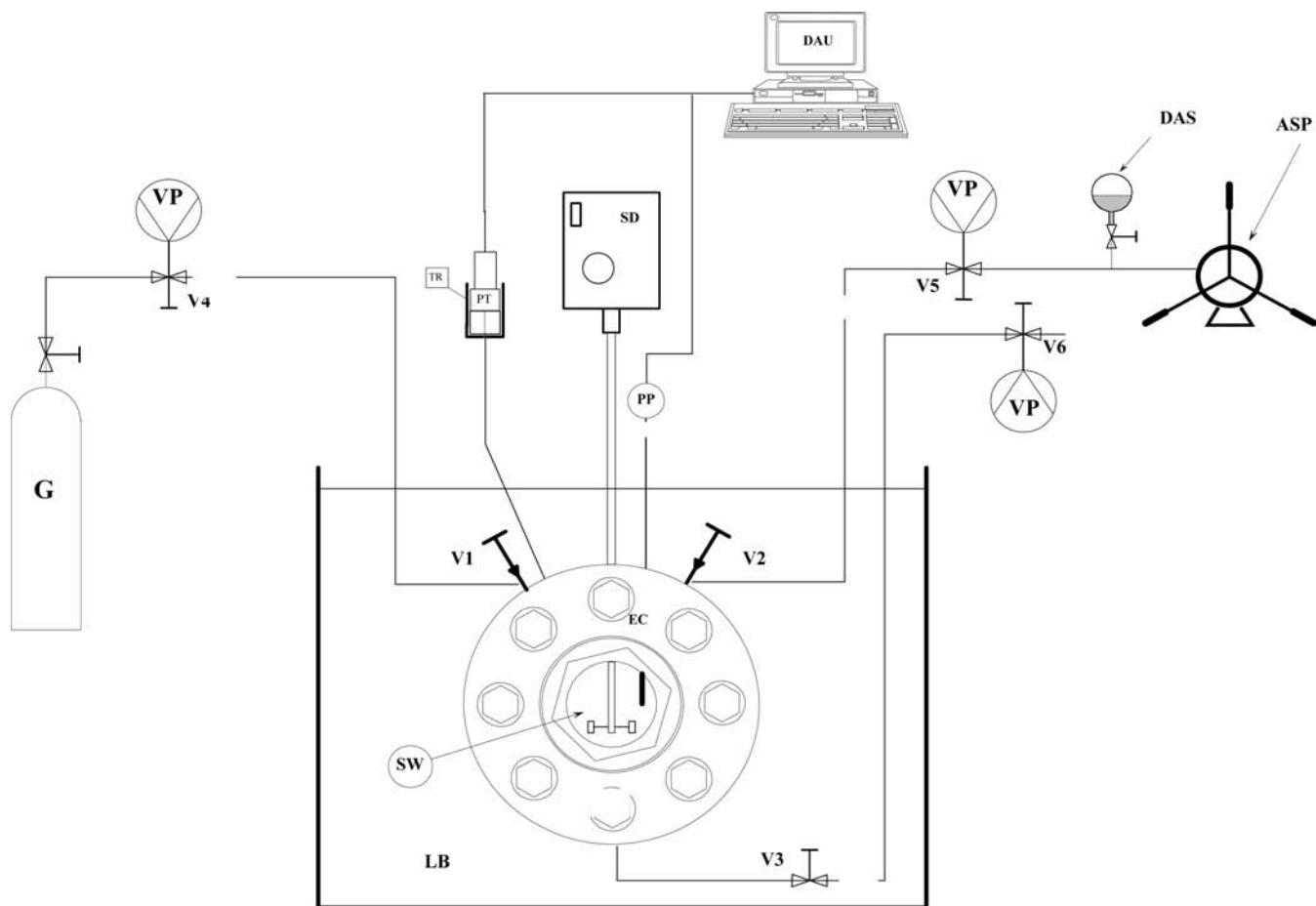


Figure 2. Schematic flow diagram of the apparatus 2. ASP, high-pressure pump; DAU, data acquisition unit; DAS, degassed aqueous solution; EC, equilibrium cell; G, gas cylinder; LB, liquid bath; PP, platinum probe; PT, “high-pressure” transducer; SD, stirring device; SW, sapphire windows, TR, temperature regulator; V1, V2, V4, V5, feeding valves; V3, V6, purge valves; VP, vacuum pump.

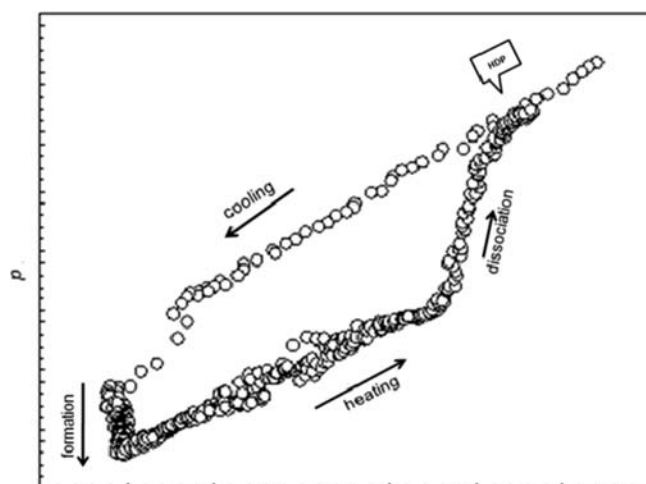


Figure 3. Typical diagram obtained using the isochoric pressure search method.^{8,9,17,41–43} T : temperature; p : pressure. The down arrow callout indicates the hydrate dissociation point (HDP).

H_2 in the presence of TBAB aqueous solutions with various concentrations available in open literature. Having investigated these reported data and the significance of the CO_2 capture

through gas hydrate technology, there is an imperative need to generate more phase equilibrium data to design the efficient processes, tuning the thermodynamic models, and investigation of the separation capabilities using semiclathrate hydrates, due to the fact that the corresponding data are still scarce. In this work, we have measured and reported such data due to two main reasons: (1) to present the experimental data at particular equilibrium temperatures and pressures and also several concentration (mass fraction) ranges of TBAB aqueous solutions, which have not been previously reported in the literature; and (2) to verify the reliability of the up to now reported experimental dissociation pressure values (indicated in Tables 1 to 4).^{8–10,17}

2. EXPERIMENTAL SECTION

Two different experimental apparatuses were used to perform the measurements.

2.1. Apparatuses. **2.1.1. Apparatus 1.** The main part of the apparatus is a cylindrical vessel made of Hastelloy, which can withstand pressures up to 20 MPa. The volume of the vessel is approximately 30 cm^3 . A magnetic stirrer is installed in the vessel to agitate the fluids and hydrate crystals inside it. A thermostatic bath (Lauda E100, Type RE112) is used to control the temperature of the equilibrium cell. Two platinum resistance thermometers (Pt100) are inserted into the vessel to measure temperatures

Table 5. Purities and Suppliers of Materials^a

material	supplier	purity
carbon dioxide	Air Liquide	0.99995 (mole fraction)
nitrogen	Air Liquide	0.99995 (mole fraction)
methane	Air Liquide	0.99995 (mole fraction)
hydrogen	Air Liquide	0.99995 (mole fraction)
TBAB (powder)	Sigma-Aldrich	0.99 (mass fraction)
TBAB	Sigma-Aldrich	0.5 mass fraction solution / aqueous solution, 0.99 (mass fraction)

^a Aqueous solutions were prepared following the gravimetric method, using an accurate analytical balance. Consequently, uncertainties on the basis of mole fraction are estimated to be < 0.01.

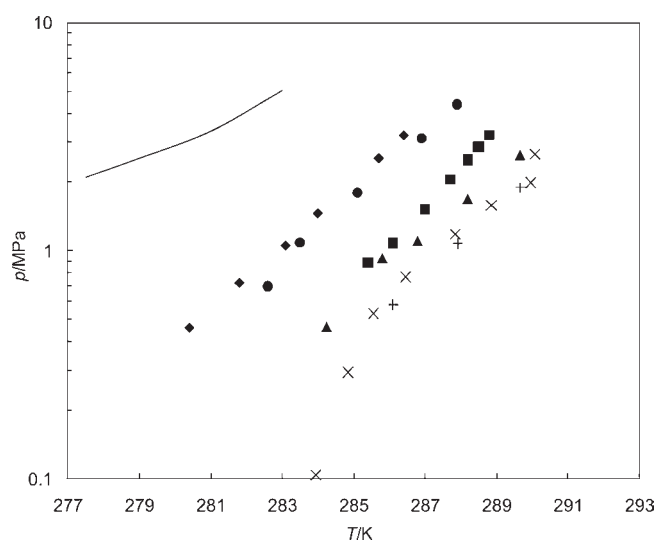


Figure 4. Experimental (this work) semiclathrate hydrate dissociation conditions for the carbon dioxide + TBAB aqueous solution. \blacklozenge , 0.050 TBAB mass fraction; \blacksquare , 0.100 TBAB mass fraction; \blacktriangle , 0.167 TBAB mass fraction; \times , 0.250 TBAB mass fraction; $+$, 0.350 TBAB mass fraction; \bullet , 0.500 TBAB mass fraction. The data including 0.250 and 0.500 TBAB mass fraction were measured applying apparatus 2, and the rest of the data were measured using apparatus 1. Curve, predictions of CSMGem hydrate model²⁵ in the presence of pure water. T : temperature; p : pressure.

and check for their equality within temperature measurement uncertainty, which is estimated to be less than 0.1 K and ensures temperature homogeneity inside the equilibrium cell. The temperature uncertainty estimation comes from calibration against a 25 Ω reference platinum resistance thermometer. The pressure in the vessel is measured with a Druck pressure transducer (Druck, type PTX611 for pressure ranges up to 16 MPa). Pressure measurement uncertainty is estimated to be less than 5 kPa, as a result of calibration against a dead weight balance (Desgranges and Huot, model 520). The schematic diagram of the experimental apparatus is shown in Figure 1.

2.1.2. Apparatus 2. The schematic diagram of this apparatus is given in Figure 2. The details of the apparatus are given elsewhere.^{8–10} The main part of the apparatus is a cylindrical equilibrium cell, made of austenite stainless steel to withstand hydrogen for embrittlement and pressures up to 60 MPa. The equilibrium cell has an inner volume of approximately 201 cm³ and two sapphire windows. A motor-driven turbine agitation system (Top Industrie) ensures sufficient agitation to facilitate

Table 6. Measured Dissociation Pressure Data for Semi-clathrate Hydrates of the Carbon Dioxide + TBAB Aqueous Solutions

w_{TBAB}^a	T^b	p^c
	K	MPa
0.050	280.4	0.462
	281.8	0.725
	283.1	1.054
	284.0	1.459
	285.7	2.540
	286.4	3.201
	285.4	0.891
	286.1	1.081
	287.0	1.523
	287.7	2.055
0.100	288.2	2.504
	288.5	2.858
	288.8	3.212
	284.2	0.464
	285.8	0.931
	286.8	1.107
	288.2	1.692
	289.7	2.637
	284.0	0.104
	284.9	0.293
0.250	285.6	0.530
	286.5	0.769
	287.9	1.178
	288.9	1.575
	290.0	1.989
	286.1	0.581
	287.9	1.074
	289.7	1.895
	282.6	0.698
	283.5	1.086
0.500	285.1	1.800
	286.9	3.104
	287.9	4.380

^a Concentration (mass fraction). ^b Temperature. ^c Pressure.

reaching equilibrium even during the hydrate formation. The temperature of the equilibrium cell is controlled using a thermostatic bath (Tamson Instruments, TV400LT), which allows the visual observation of the cell content throughout the experiments. One platinum resistance sensor (Pt100) inserted in the cell interior is used in situ to measure the temperature having less than 0.1 K uncertainty estimated after calibration against a 25 Ω reference platinum resistance thermometer. This 25 Ω reference probe was calibrated, following the ITS 90 protocol, by Laboratoire National d'essais (Paris). The pressure is measured using a pressure transducer (Druck, type PTX611) for pressures up to 40 MPa. As a result of calibration against a dead weight balance (Desgranges & Huot S202S CP, Aubervilliers, France), the pressure uncertainty is estimated to be less than 5 kPa.

2.2. Common Experimental Procedure. The hydrate dissociation conditions were measured (applying both apparatuses)

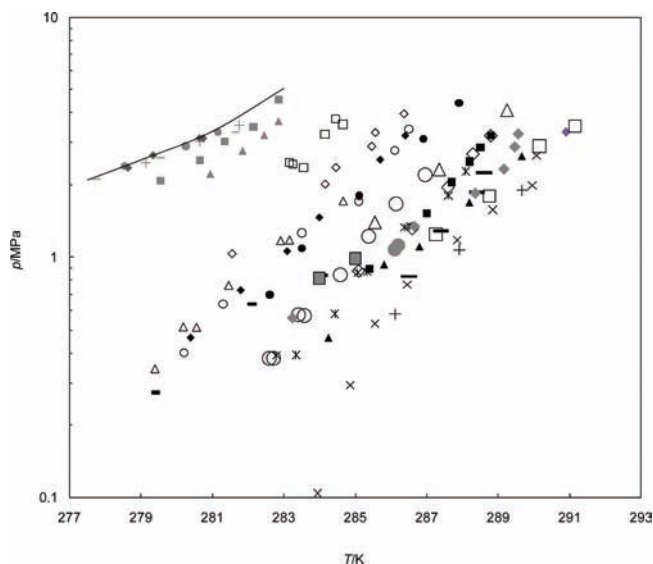


Figure 5. Experimental semiclathrate hydrate dissociation conditions for the carbon dioxide + TBAB aqueous solutions. This work: \blacklozenge , 0.050 TBAB mass fraction; \blacksquare , 0.100 TBAB mass fraction; \blacktriangle , 0.167 TBAB mass fraction; \times , 0.250 TBAB mass fraction; $+$, 0.350 TBAB mass fraction; \bullet , 0.50 TBAB mass fraction. Literature: gray \blacktriangle ,⁴⁸ 0.02 TBAB mass fraction; large \circ ,⁴⁹ 0.0702 TBAB mass fraction; \square ,⁴⁷ 0.427 TBAB mass fraction; large \triangle ,⁴⁹ 0.443 TBAB mass fraction; small \diamond ,⁴⁸ 0.045 TBAB mass fraction; gray \bullet ,⁴⁸ 0.01 TBAB mass fraction; gray \blacksquare ,⁴⁸ 0.01 TBAB mass fraction; $-$,⁴⁸ 0.03 TBAB mass fraction; $-$,¹⁴ 0.05 TBAB mass fraction; $+$,⁴⁸ 0.02 TBAB mass fraction; large \diamond ,⁵⁰ 0.10 TBAB mass fraction; bold black line,³⁸ 0.40 TBAB mass fraction; small \circ ,⁵⁰ 0.05 TBAB mass fraction; $*$,⁴⁹ 0.0901 TBAB mass fraction; small \triangle ,⁴⁷ 0.10 mass fraction; bold gray line,⁴⁸ 0.045 TBAB mass fraction. Curve, predictions of CSMGem hydrate model²⁵ in the presence of pure water. T : temperature; p : pressure.

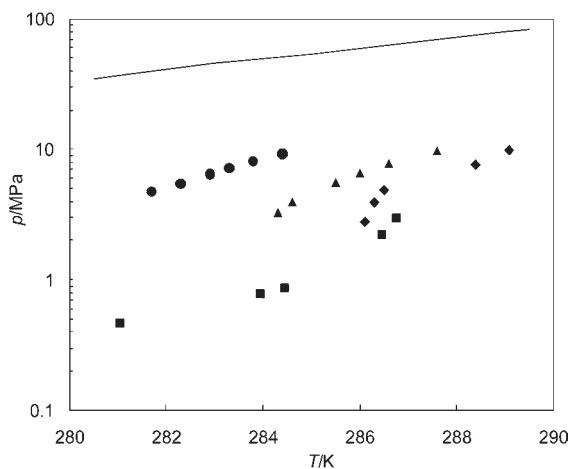


Figure 6. Experimental (this work) semiclathrate hydrate dissociation conditions for the nitrogen + TBAB aqueous solution. \bullet , 0.050 TBAB mass fraction; \blacktriangle , 0.100 TBAB mass fraction; \blacklozenge , 0.500 TBAB mass fraction; \blacksquare , 0.250 TBAB mass fraction. The data including 0.250 and 0.500 TBAB mass fraction were measured using apparatus 2, and the rest of the data were measured using apparatus 1. Curve, predictions of CSMGem hydrate model²⁵ in the presence of pure water. T : temperature; p : pressure.

through an isochoric pressure search method^{18,9,17,41–44} as implemented by Ohmura and co-workers.⁴² The reliability of this method

Table 7. Dissociation Conditions for Semiclathrate Hydrates of the Nitrogen + TBAB Aqueous Solution

w_{TBAB}^a	T^b		p^c
	K		
0.050	281.7		4.710
	282.3		5.450
	282.9		6.460
	283.3		7.180
	283.8		8.110
	284.4		9.250
0.100	284.3		3.310
	284.6		3.980
	285.5		5.620
	286.0		6.610
	286.6		7.820
	287.6		9.790
0.250	281.1		0.470
	284.0		0.780
	284.5		0.870
	286.5		2.190
	286.8		3.000
	286.1		2.790
0.500	286.3		3.930
	286.5		4.885
	288.4		7.670
	289.1		9.920

^a Concentration (mass fraction). ^b Temperature. ^c Pressure.

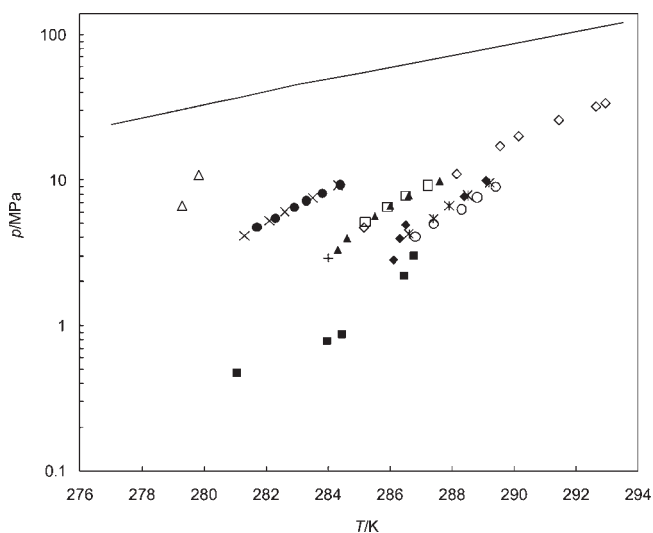


Figure 7. Experimental semiclathrate hydrate dissociation conditions for the nitrogen + TBAB aqueous solution. This work: \bullet , 0.050 TBAB mass fraction; \blacktriangle , 0.100 TBAB mass fraction; \blacklozenge , 0.500 TBAB mass fraction; \blacksquare , 0.250 TBAB mass fraction. Literature: \circ ,¹⁶ 0.40 TBAB mass fraction; \square ,¹⁶ 0.60 TBAB mass fraction; \triangle ,¹⁴ 0.05 TBAB mass fraction; \diamond ,⁴⁷ 0.10 TBAB mass fraction; $+$,¹⁴ 0.10 TBAB mass fraction; \times ,¹⁶ 0.05 TBAB mass fraction; $*$,¹⁶ 0.20 TBAB mass fraction. Curve, predictions of CSMGem hydrate model²⁵ in the presence of pure water. T : temperature; p : pressure.

has been previously demonstrated.^{8–10,17,41–44} The vessel containing aqueous solution (approximately 10 % by volume of the

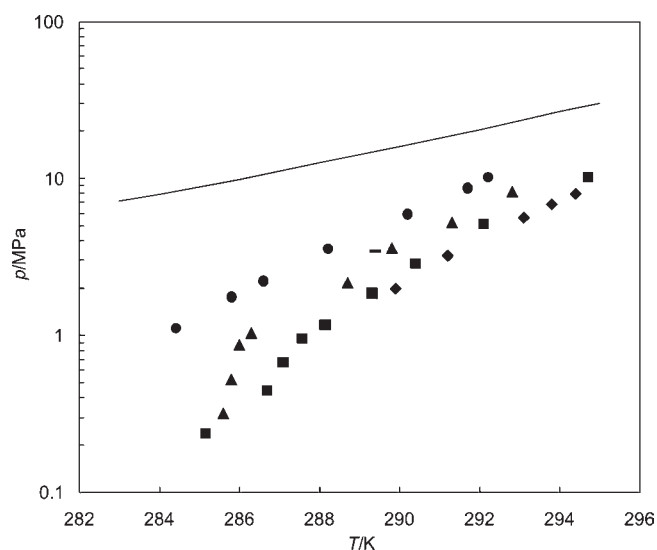


Figure 8. Experimental (this work) semiclathrate hydrate dissociation conditions for the methane + TBAB aqueous solution. ●, 0.100 TBAB mass fraction; line, 0.153 TBAB mass fraction; ▲, 0.500 TBAB mass fraction; ■, 0.250 TBAB mass fraction; ◆, 0.350 TBAB mass fraction. The data including 0.250 and 0.500 TBAB mass fraction were measured using apparatus 2, and the rest of the data were measured using apparatus 1. Curve, predictions of CSMGem hydrate model²⁵ in the presence of pure water. *T*: temperature; *p*: pressure.

vessel was filled with aqueous solution) was immersed into the temperature-controlled bath, and the gas was supplied from a cylinder through a pressure-regulating valve into the vessel. Note that the vessel was evacuated before the introduction of any aqueous solution and gas. After obtaining temperature and pressure stability (far enough from the hydrate formation region), the valve in the line connecting the vessel and the cylinder was closed. Subsequently, temperature was slowly decreased to form the hydrate. Hydrate formation in the vessel was observed when a pressure drop at constant temperature was detected using the data acquisition unit. The temperature was then increased with steps of 0.1 K. At every temperature step, the temperature was kept constant with enough time to obtain an equilibrium state in the cell. Therefore, a pressure–temperature diagram was sketched for each experimental run, from which we determined the hydrate dissociation point.^{8,9,17,41–44} During the dissociation of the hydrate crystals inside hydrate formation region, the pressure is gradually increased by increasing the temperature. However, outside this region, a slight pressure increase is observed during the increase of temperature.^{8–10,17,41–44} Consequently, the hydrate dissociation point can be determined when the slope of the pressure–temperature diagram changes suddenly.^{8,9,17,41–44} A typical diagram of this experimental method is shown in Figure 3. The uncertainties for the hydrate dissociation temperatures and pressures are expected to be ± 0.1 K and ± 0.020 MPa based on our previous studies. Furthermore, Table 5 shows the materials used in this work.

3. RESULTS AND DISCUSSION

The measured dissociation conditions of semiclathrate hydrates of CO₂ in the presence of 0.050, 0.100, 0.167, 0.250, 0.350, and 0.500 mass fraction of TBAB aqueous solutions are reported in Figure 4 and Table 6. A semilogarithmic scale has been used in

Table 8. Dissociation Conditions for Semiclathrate Hydrates of the Methane + TBAB Aqueous Solution

w_{TBAB}^a	T^b		p^c	
	K			MPa
0.100	284.4		1.112	
	285.8		1.754	
	286.6		2.221	
	288.2		3.562	
	290.2		5.923	
	291.7		8.713	
	292.2		10.158	
	289.4		3.471	
	0.153	285.1		0.235
		286.7		0.444
0.250	287.1		0.678	
	287.6		0.954	
	288.1		1.171	
	289.3		1.848	
	290.4		2.888	
	292.1		5.124	
	294.7		10.217	
	0.350	289.9		1.979
		291.2		3.223
		293.1		5.648
293.8		6.892		
294.4		8.036		
0.500		285.6		0.317
		285.8		0.522
		286.0		0.868
		286.3		1.036
		288.7		2.166
	289.8		3.596	
	291.3		5.247	
	292.8		8.260	

^a Concentration (mass fraction). ^b Temperature. ^c Pressure.

this figure to show the data consistency. The predictions of the CSMGem hydrate model,²⁵ which is an accurate model for determination of the phase equilibria of pure hydrate formers in the presence of pure water, are also indicated in Figure 4. This model, which is based on the Gibbs energy minimization, has been developed taking into account the principles of the phase equilibrium criteria.²⁵ It allows for calculations of the formation conditions for any phase (including the hydrate phase).

Moreover, Figure 5 shows a comparison between our obtained data and the experimental phase equilibrium data for semiclathrate hydrates of CO₂ in the presence of TBAB aqueous solutions, reported in the literature. As can be seen, TBAB has drastic promotion effects that is, the formation conditions of the clathrate hydrates of CO₂ in the presence of pure water are shifted to the higher temperatures and lower pressures. Furthermore, our data at TBAB concentrations of 0.050 and 0.100 (mass fraction) are in acceptable agreement with the literature data.

However, the promotion effects of TBAB aqueous solutions are more sensible at low concentrations of TBAB aqueous solutions (based on mass fraction). In other words, by increasing the amount of TBAB in the aqueous solutions, the shift in

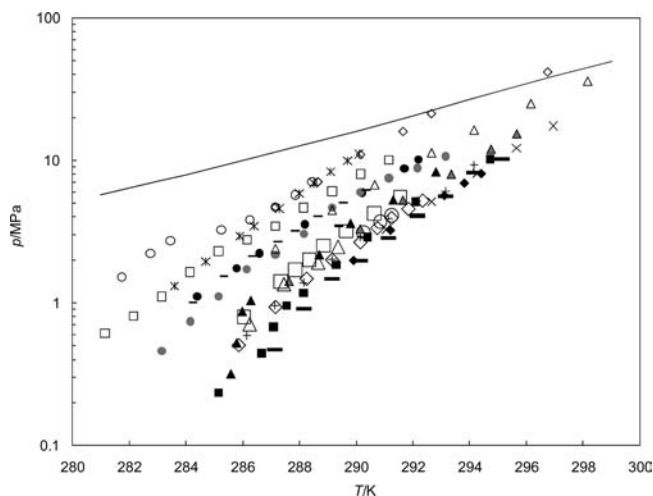


Figure 9. Experimental semiclathrate hydrate dissociation conditions for the methane + TBAB aqueous solution. This work: ●, 0.100 TBAB mass fraction; line, 0.153 TBAB mass fraction; ▲, 0.500 TBAB mass fraction; ■, 0.250 TBAB mass fraction; ◆, 0.350 TBAB mass fraction. Literature: gray ▲,⁵⁰ 0.20 TBAB mass fraction; large ○,⁵² 0.45 TBAB mass fraction; □,⁵² 0.20 TBAB mass fraction; large △,⁵² 0.45 TBAB mass fraction; small ◇,⁴⁷ 0.05 TBAB mass fraction; gray ●,⁵⁰ 0.099 TBAB mass fraction; −,⁵⁰ 0.05 TBAB mass fraction; −,⁵² 0.10 TBAB mass fraction; +,⁵⁰ 0.197 TBAB mass fraction; large ◇,⁵² 0.288 TBAB mass fraction; bold black line,⁵⁰ 0.385 TBAB mass fraction; small ○,⁵² 0.05 TBAB mass fraction; *,⁵¹ 0.05 TBAB mass fraction; small △,⁴⁷ 0.10 mass fraction; ×,⁵⁰ 0.30 TBAB mass fraction. Curve, predictions of CSMGem hydrate model²⁵ in the presence of pure water. *T*: temperature; *p*: pressure.

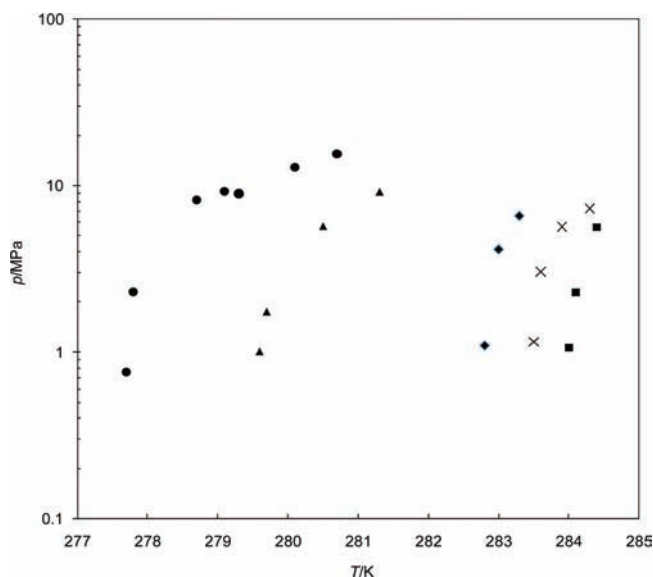


Figure 10. Experimental (this work) semiclathrate hydrate dissociation conditions for the hydrogen + TBAB aqueous solution. ●, 0.050 TBAB mass fraction; ▲, 0.100 TBAB mass fraction; ◆, 0.150 TBAB mass fraction; ×, 0.200 TBAB mass fraction; ■, 0.250 TBAB mass fraction. The presented data were measured using apparatus 2. *T*: temperature; *p*: pressure.

temperature and pressure conditions of the carbon dioxide hydrate formation is reduced. On the other hand, adding more TBAB to the system after a particular concentration of this promoter in aqueous solution (about 0.4 mass fraction)^{45–47} has a contradictory effect

Table 9. Dissociation Conditions for Semiclathrate Hydrates of the Hydrogen + TBAB Aqueous Solution

w_{TBAB}^a	T^b		p^c
	K		
0.050	277.7		0.760
	277.8		2.280
	278.7		8.160
	279.1		9.190
	279.3		8.930
	280.1		12.870
	280.7		15.490
0.100	279.6		1.010
	279.7		1.750
	280.5		5.660
	281.3		9.110
0.150	282.8		1.103
	283.0		4.132
	283.3		6.563
0.200	283.5		1.160
	283.6		3.020
	283.9		5.650
	284.3		7.270
	284.0		1.070
	284.1		2.280
0.250	284.4		5.570

^a Concentration (mass fraction). ^b Temperature. ^c Pressure.

(inhibition effect) for gas hydrate formation. Another point is that the reported dissociation pressure data including those of Arajmami et al.⁴⁷ and Lin et al.,⁴⁹ which are related to the concentrations above the stoichiometric ratios, also prove this phenomenon. Moreover, these data are in acceptable agreement with each other and also our data for this phase equilibrium region.

The obtained experimental semiclathrate hydrate dissociation data for the system N_2 + TBAB aqueous solution at different concentrations of TBAB (mass fraction) are reported in Figure 6 and Table 7. Figure 7 shows a comparison between the measured hydrate dissociation data in this work and almost all of dissociation conditions of semiclathrate hydrates of N_2 in the presence of different concentrations (mass fraction) of TBAB aqueous solutions reported in the literature. This figure clearly shows some disagreements among our data and the reported ones in the literature. For instance, the equilibrium data at 0.50 mass fraction of TBAB aqueous solution provided by Duc et al.¹⁴ overlap those data of Lee et al.¹⁶ and also our data. This fact reveals the necessity of significant care that should be taken into account in measuring the equilibrium pressures of semiclathrate hydrates especially due to the fact that a small increase in temperature generally contributes to a large shift in dissociation pressure in comparison with the hydrates formed in the presence of pure water. Figure 7 also indicates that the effects of adding aqueous solutions containing 0.600 mass fraction of TBAB on the equilibrium conditions of the investigated system seem to be the same as the addition of the aqueous solutions containing 0.100 mass fraction of TBAB.

The results of the semiclathrate hydrate dissociation conditions for the system of CH_4 + TBAB (0.050, 0.100, 0.153, 0.250, 0.350, and 0.500 mass fraction) aqueous solutions are obtained in this work shown in Figure 8 and Table 8. A comparison between

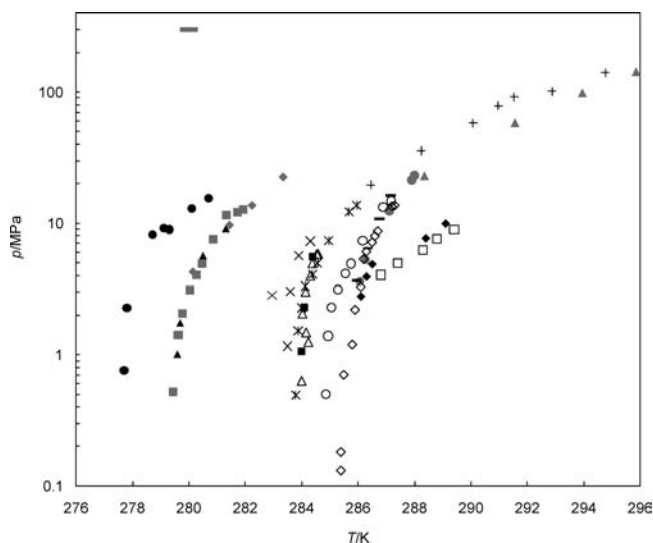


Figure 11. Experimental semicathrate hydrate dissociation conditions for the hydrogen + TBAB aqueous solution. This work: ●, 0.050 TBAB mass fraction; ▲, 0.100 TBAB mass fraction; ×, 0.200 TBAB mass fraction; ■, 0.250 TBAB mass fraction; ◆, 0.50 TBAB mass fraction. Literature: gray ▲,⁵⁵ 0.4074 TBAB mass fraction; ○,⁵⁴ 0.5738 TBAB mass fraction; □,¹⁶ 0.40 TBAB mass fraction; △,⁴⁸ 0.25 TBAB mass fraction; ◇,⁵³ 0.401 TBAB mass fraction; gray ●,⁴⁷ 0.43 TBAB mass fraction; bold black line,⁵⁶ 0.037 TBAB mass fraction; +,⁵⁵ 0.2674 TBAB mass fraction; *,⁵⁴ 0.2674 TBAB mass fraction; gray ■,⁵⁴ 0.0975 TBAB mass fraction; gray ◆,⁴⁷ 0.1 TBAB mass fraction; bold gray line,⁵⁷ without TBAB. *T*: temperature; *p*: pressure.

these obtained data and the data reported in the literature is indicated in Figure 9. Acceptable agreement is found between our data and the existing data in open literature. For example, at a near stoichiometric ratio, where the measurements should be done very carefully, our data (at 0.350 mass fraction of TBAB) and the reported data by Li et al.⁵⁰ (at 0.385 mass fraction of TBAB) show an acceptable agreement. Furthermore, a similar conclusion can be made about the inhibition effect of TBAB above its stoichiometric ratio in the aqueous phase. However, there is an evident disagreement between the reported data in the literature. The data provided by Sun and Sun⁵² in the presence of 0.05 mass fraction of TBAB aqueous solutions do not coincide well with those of Mohammadi and Richon⁵¹ at lower temperatures, that is, below 286 K.

Finally, the measured phase equilibrium data for the semicathrate hydrate of H₂ in the presence of different TBAB aqueous solutions are reported in Figure 10 and Table 9. It can be concluded that the main promotion effect of TBAB seems to be with addition of TBAB aqueous solutions between 0.100 and 0.150 mass fraction of TBAB. However, the shift in equilibrium temperature and pressure conditions is gradually decreased when reaching the stoichiometric ratio. Figure 11 shows a comparison between our measured data with the available data in open literature. Because the CSMGem thermodynamic hydrate model²⁵ has not been extended for calculations of equilibrium conditions of gas hydrates of hydrogen in the presence of pure water, we have indicated the corresponding data provided by Mao and Mao⁵⁷ in Figure 11 for comparison purposes. Furthermore, the phase behaviors of the semicathrate hydrates of hydrogen + TBAB seem to be slightly different than the other three investigated ones especially when the equilibrium pressures are sketched in

semilogarithmic scale. However, it is evident that the addition of TBAB aqueous solution to the system greatly shifts the pressure-temperature conditions of the Lw-H-V (liquid water–hydrate–vapor) equilibrium of such a system.

4. CONCLUSION

In this work, we presented comprehensive semicathrate hydrate dissociation data in the (277.7 to 294.7) K temperature range and pressures up to 15.49 MPa for the systems including CO₂, N₂, CH₄, or CO₂ + TBAB aqueous solutions with different concentrations (0.050, 0.100, 0.150, 0.153, 0.167, 0.250, 0.350, and 0.500 mass fraction). Two in-house designed and built apparatuses were used for the experimental measurements, which were performed based on an isochoric pressure search technique.^{8,9,17,41–44} It was inferred that, after a particular stoichiometric ratio, the addition of TBAB has an inhibition effect on gas hydrate formation. Moreover, the promotion effects of TBAB aqueous solutions are more sensible at low concentrations (mass fraction) of TBAB aqueous solutions. A comparison between our experimental data with those ones presented in the literature shows some disagreements, which reveal the importance of measurements of corresponding phase equilibrium data. The reported data are of much interest for designing special separation processes of CO₂ from the flue and industrial gases.

■ AUTHOR INFORMATION

Corresponding Author

*E-mail: amir-hosseini.mohammadi@mines-paristech.fr. Tel.: + (33) 1 64 69 49 70. Fax: + (33) 1 64 69 49 68.

Funding Sources

This work was financially supported by the Agence Nationale de la Recherche (ANR) as part of the SECOHYA project. The financial support of Orientation Stratégique des Ecoles des Mines (OSEM) is also acknowledged. A.E. is grateful to Mines ParisTech for providing him a Ph.D. scholarship. V.B. acknowledges Fundayacucho of Venezuela for providing her a Ph.D. scholarship.

■ REFERENCES

- (1) Englezos, P.; Lee, J. D. Gas hydrates: A cleaner source of energy and opportunity for innovative technologies. *Korean J. Chem. Eng.* **2005**, *22*, 671–681.
- (2) Bacher, P. Meeting the Energy Challenges of the 21st Century. *Int. J. Energy Technol. Policy* **2002**, *1*.
- (3) Hall, C.; Tharakan, P.; Hallock, J.; Cleveland, C.; Jefferson, M. Hydrocarbons and the evolution of human culture. *Nature* **2003**, *426*, 318–322.
- (4) *Carbon dioxide capture and storage*; Special Report for the International Panel on Climate (IPCC): Geneva, February 5, 2007. Climate Change 2007: The Physical Science Basis - Summary for Policy Makers. <http://www.ipcc.ch/SPM2feb07.pdf>.
- (5) Gough, C.; Shackley, S.; Cannell, M. G. R. *Evaluating the options for carbon sequestration*; Tyndall Centre for Climate Change Research, Technical Report 2, UMIST: Manchester, 2002.
- (6) Rau, G. CO₂ mitigation via capture and chemical conversion in seawater. *Environ. Sci. Technol.* **2011**, *45*, 1088–1092.
- (7) Saha, D.; Bao, Z.; Jia, F.; Deng, S. Adsorption of CO₂, CH₄, N₂O, and N₂ on MOF-5, MOF-177, and Zeolite 5A. *Environ. Sci. Technol.* **2010**, *44*, 1820–1826.
- (8) Belandria, V.; Eslamimanesh, A.; Mohammadi, A. H.; Théveneau, P.; Legendre, H.; Richon, D. Compositional analysis and hydrate

dissociation conditions measurements for carbon dioxide + methane + water system. *Ind. Eng. Chem. Res.* **2011**, *50*, 5783–5794.

(9) Belandria, V.; Eslamimanesh, A.; Mohammadi, A. H.; Richon, D. Gas hydrate formation in carbon dioxide + nitrogen + water system: Compositional analysis of equilibrium phases. *Ind. Eng. Chem. Res.* **2011**, *50*, 4722–4730.

(10) Belandria, V.; Eslamimanesh, A.; Mohammadi, A. H.; Richon, D. Study of gas hydrate formation in carbon dioxide + hydrogen + water system: Compositional analysis of gas phase. *Ind. Eng. Chem. Res.* **2011**, *50*, 6455–6459.

(11) Feron, P. H. M.; Hendricks, C. A. CO₂ capture process principles and costs. *Oil Gas Sci. Technol.* **2005**, *60*, 451–459.

(12) Kang, S. P.; Lee, H. Recovery of CO₂ from flue gas using gas hydrate: Thermodynamic verification through phase equilibrium measurements. *Environ. Sci. Technol.* **2000**, *34*, 4397–4400.

(13) Linga, P.; Kumar, R.; Englezos, P. The clathrate hydrate process for post and pre-combustion capture of carbon dioxide. *J. Hazard. Mater.* **2007**, *149*, 625–629.

(14) Duc, N. H.; Chauvy, F.; Herri, J. M. CO₂ capture by hydrate crystallization - A potential solution for gas emission of steelmaking industry. *Energy Convers. Manage.* **2007**, *48*, 1313–1322.

(15) Kumar, R.; Wu, H. J.; Englezos, P. Incipient hydrate phase equilibrium for gas mixtures containing hydrogen, carbon dioxide and propane. *Fluid Phase Equilib.* **2006**, *244*, 167–171.

(16) Lee, H. J.; Lee, J. D.; Linga, P.; Englezos, P.; Kim, Y. S.; Lee, M. S.; Kim, Y. D. Gas hydrate formation process for pre-combustion capture of carbon dioxide. *Energy* **2010**, *35*, 2729–2733.

(17) Semiclathrate hydrate phase equilibrium measurements for CO₂ + N₂ + tetra-n-butylammonium bromide aqueous solutions. Private communication, 2011.

(18) Seo, Y. T.; Kang, S. P.; Lee, H.; Lee, C. S.; Sung, W. M. Hydrate Phase Equilibria for Gas Mixtures Containing Carbon Dioxide: A Proof-of-Concept to Carbon Dioxide Recovery from Multicomponent Gas Stream. *Korean J. Chem. Eng.* **2000**, *17*, 659–667.

(19) Zhao, J. Z.; Zhao, Y. S.; Shi, D. X. Experiment on methane concentration from oxygen-containing coal bed gas by THF solution hydrate formation. *Meitan Xuebao* **2008**, *33*, 1419–1424.

(20) United States Environmental Protection Agency: Washington, DC, 2011. <http://www.epa.gov>.

(21) Eslamimanesh, A.; Mohammadi, A. H.; Richon, D. Thermodynamic consistency test for experimental data of water content of methane. In press. *AIChE J.* **2011** DOI: 10.1002/aic.12462.

(22) Zhang, B. Y.; Wu, Q.; Zhu, Y. M. Effect of THF on the thermodynamics of low-concentration gas hydrate formation. *Zhongguo Kuangye Daxue Xuebao* **2009**, *38*, 203–208.

(23) Sun, C. Y.; Ma, C. F.; Chen, G. J.; Zhang, S. X. Experimental and simulation of single equilibrium stage separation of (methane + hydrogen) mixtures via forming hydrate. *Fluid Phase Equilib.* **2007**, *261*, 85–91.

(24) United States Climate Change Science Program: Washington, DC, www.globalchange.gov 2011.

(25) Sloan, E. D.; Koh, C. A. *Clathrate Hydrates of Natural Gases*, 3rd ed.; CRC Press, Taylor & Francis Group: New York, 2008.

(26) Eslamimanesh, A.; Mohammadi, A. H.; Richon, D. An improved Clapeyron model for predicting liquid water-hydrate-liquid hydrate former phase equilibria. *Chem. Eng. Sci.* **2011**, *66*, 1759–1764.

(27) Kim, D. Y.; Lee, H. Spectroscopic identification of the mixed hydrogen and carbon dioxide clathrate hydrate. *J. Am. Chem. Soc.* **2005**, *127*, 9996–9997.

(28) Papadimitriou, N. I.; Tsimpanogiannis, I. N.; Stubos, A. K.; Martin, A.; Rovetto, L. J.; Florusse, L. J.; Peters, C. J. Experimental and computational investigation of the sII Binary He-THF hydrate. *J. Phys. Chem. B* **2011**, *115*, 1411–1415.

(29) Sabil, K. M.; Nadia, O.; Witkamp, G.; Peters, C. J.; Bruining, J. M. Hydrate-Aqueous Liquid-Vapor Equilibrium (H-L_W-V) for binary CO₂/H₂ mixture in aqueous solutions of water and tetrahydrofuran. *Proc. Int. Conf. Chem. Eng. Appl.* **2010**, 171–175.

(30) Sabil, K. M.; Duarte, A. R. C.; Zevenbergen, J.; Ahmad, M. M.; Yusup, S.; Omar, A. A.; Peters, C. J. Kinetic of formation for single

carbon dioxide and mixed carbon dioxide and tetrahydrofuran hydrates in water and sodium chloride aqueous solution. *Int. J. Greenhouse Gas Control* **2010**, *4*, 798–805.

(31) Sabil, K. M.; Witkamp, G. J.; Peters, C. J. Phase equilibria in ternary (carbon dioxide + tetrahydrofuran + water) system in hydrate-forming region: Effects of carbon dioxide concentration and the occurrence of pseudo-retrograde hydrate phenomenon. *J. Chem. Thermodyn.* **2010**, *42*, 8–16.

(32) Mooijer-Van Den Heuvel, M. M.; Witteman, R.; Peters, C. J. Phase behaviour of gas hydrates of carbon dioxide in the presence of tetrahydrofuran, cyclobutanone, cyclohexane and methylcyclohexane. *Fluid Phase Equilib.* **2001**, *182*, 97–110.

(33) Strobel, T. A.; Hester, K. C.; Koh, C. A.; Sum, A. K.; Sloan, E. D., Jr. Properties of the clathrates of hydrogen and developments in their applicability for hydrogen storage. *Chem. Phys. Lett.* **2009**, *478*, 97–109.

(34) Strobel, T. A.; Koh, C. A.; Sloan, E. D. Thermodynamic predictions of various tetrahydrofuran and hydrogen clathrate hydrates. *Fluid Phase Equilib.* **2009**, *280*, 61–67.

(35) Shin, K.; Kim, Y.; Strobel, T. A.; Prasad, P. S. R.; Sugahara, T.; Lee, H.; Sloan, E. D.; Sum, A. K.; Koh, C. A. Tetra-n-butylammonium borohydride semiclathrate: A hybrid material for hydrogen storage. *J. Phys. Chem. A* **2009**, *113*, 6415–6418.

(36) Makino, T.; Yamamoto, T.; Nagata, K.; Sakamoto, H.; Hashimoto, S.; Sugahara, T.; Ohgaki, K. Thermodynamic stabilities of tetra-n-butyl ammonium chloride + H₂, N₂, CH₄, CO₂, or C₂H₆ semiclathrate hydrate systems. *J. Chem. Eng. Data* **2010**, *55*, 839–841.

(37) Wenji, S.; Rui, X.; Chong, H.; Shihui, H.; Kaijun, D.; Ziping, F. Experimental investigation on TBAB clathrate hydrate slurry flows in a horizontal tube: Forced convective heat transfer behaviors. *Int. J. Refrig.* **2009**, *32* (7), 1801–1807.

(38) Deschamps, J.; Dalmazzone, D. Dissociation enthalpies and phase equilibrium for TBAB semi-clathrate hydrates of N₂, CO₂, N₂ + CO₂ and CH₄ + CO₂. *J. Therm. Anal. Calorim.* **2009**, *98*, 113–118.

(39) Fan, S.; Li, S.; Wang, J.; Lang, X.; Wang, Y. Efficient capture of CO₂ from simulated flue gas by formation of TBAB or TBAF semiclathrate hydrates. *Energy Fuels* **2009**, *23*, 4202–4208.

(40) Eslamimanesh, A.; Mohammadi, A. H.; Belandria, V.; Richon, D. ANR SECOHYA project; Internal Progress Report, January 2011.

(41) Tohidi, B.; Burgass, R. W.; Danesh, A.; Ostergaard, K. K.; Todd, A. C. Improving the accuracy of gas hydrate dissociation point measurements. *Ann. N.Y. Acad. Sci.* **2000**, *912*, 924–931.

(42) Ohmura, R.; Takeya, S.; Uchida, T.; Ebinuma, T. Clathrate hydrate formed with methane and 2-Propanol: Confirmation of structure II hydrate formation. *Ind. Eng. Chem. Res.* **2004**, *43*, 4964–4966.

(43) Mohammadi, A. H.; Afzal, W.; Richon, D. Experimental data and predictions of dissociation conditions for ethane and propane simple hydrates in the presence of distilled water and methane, ethane, propane, and carbon dioxide simple hydrates in the presence of ethanol aqueous solutions. *J. Chem. Eng. Data* **2008**, *53*, 683–686.

(44) Tumba, K.; Reddy, P.; Naidoo, P.; Ramjugernath, D.; Eslamimanesh, A.; Mohammadi, A. H.; Richon, D. Phase equilibria of methane and carbon dioxide clathrate hydrates in the presence of aqueous solutions of tributylmethylphosphonium methylsulfate ionic liquid. *J. Chem. Eng. Data* **2011**, DOI: 10.1021/je200462q.

(45) Shimada, W.; Ebinuma, T.; Oyama, H.; Kamata, Y.; Takeya, S.; Uchida, T.; Nagao, J.; Narita, H. Separation of gas molecule using tetra-n-butyl ammonium bromide semi-clathrate hydrate crystals. *Jpn. J. Appl. Phys., Part 2: Lett.* **2003**, *42*, L129–L131.

(46) Fukushima, S.; Takao, S.; Ogoshi, H.; Ida, H.; Matsumoto, S.; Akiyama, T.; Otsuka, T. Development of high-density cold latent heat with clathrate hydrate, NKK Tech. Report (in Japanese); JFE Steel corporation, 1999; Vol. 166, pp 65–70.

(47) Arjmandi, M.; Chapoy, A.; Tohidi, B. Equilibrium data of hydrogen, methane, nitrogen, carbon dioxide, and natural gas in semi-clathrate hydrates of tetrabutyl ammonium bromide. *J. Chem. Eng. Data* **2007**, *52*, 2153–2158.

(48) Oyama, H.; Ebinuma, T.; Nagao, J.; Narita, H.; Shimada, W. *Phase Behavior of TBAB Semiclathrate Hydrate Crystal Under Several*

Vapor Components, Proceedings of the 6th International Conference on Gas Hydrates (ICGH), Vancouver, Canada, 2008.

(49) Lin, W.; Delahaye, A.; Fournaison, L. Phase equilibrium and dissociation enthalpy for semi-clathrate hydrate of CO₂ + TBAB. *Fluid Phase Equilib.* **2008**, *264*, 220–227.

(50) Li, S.; Fan, S.; Wang, J.; Lang, X.; Wang, Y. Clathrate hydrate capture of CO₂ from simulated flue gas with cyclopentane/water emulsion. *Chin. J. Chem. Eng.* **2010**, *18*, 202–206.

(51) Mohammadi, A. H.; Richon, D. Phase equilibria of semi-clathrate hydrates of tetra-n-butylammonium bromide + hydrogen sulfide and tetra-n-butylammonium bromide + methane. *J. Chem. Eng. Data* **2010**, *55*, 982–984.

(52) Sun, Z. G.; Sun, L. Equilibrium conditions of semi-clathrate hydrate dissociation for methane + tetra-n-butyl ammonium bromide. *J. Chem. Eng. Data* **2010**, *55*, 3538–3541.

(53) Hashimoto, S.; Murayama, S.; Sugahara, T.; Sato, H.; Ohgaki, K. Thermodynamic and Raman spectroscopic studies on H₂ + tetrahydrofuran + water and H₂ + tetra-n-butyl ammonium bromide + water mixtures containing gas hydrates. *Chem. Eng. Sci.* **2006**, *61*, 7884–7888.

(54) Hashimoto, S.; Sugahara, T.; Moritoki, M.; Sato, H.; Ohgaki, K. Thermodynamic stability of hydrogen + tetra-n-butyl ammonium bromide mixed gas hydrate in nonstoichiometric aqueous solutions. *Chem. Eng. Sci.* **2008**, *63*, 1092–1097.

(55) Hashimoto, S.; Tsuda, T.; Ogata, K.; Sugahara, T.; Inoue, Y.; Ohgaki, K. Thermodynamic properties of hydrogen + tetra-n-butyl ammonium bromide semi-clathrate hydrate. *J. Thermodyn.* **2010**, Article ID 170819, 1–5.

(56) Chapoy, A.; Burgass, R.; Tohidi, B.; Austell, J. M.; Eickhoff, C. Effect of common impurities on the phase behaviour of carbon dioxide rich systems: Minimizing the risk of hydrate formation and two-phase flow. *SPE J.* **2009**, SPE 123778-MS.

(57) Mao, W. L.; Mao, H. K. Hydrogen storage in molecular compounds. *Proc. Natl. Acad. Sci. U.S.A.* **2004**, *101*, 708–710.